

Supporting Material for

LIVER-SELECTIVE MMP-9 INHIBITION REDUCES INJURY AND ACCELERATES LIVER REGENERATION

Xiangdong Wang, Ana C. Maretti-Mira, Lei Wang, Laurie D. DeLeve

correspondence to: deleve@med.usc.edu

This file includes:

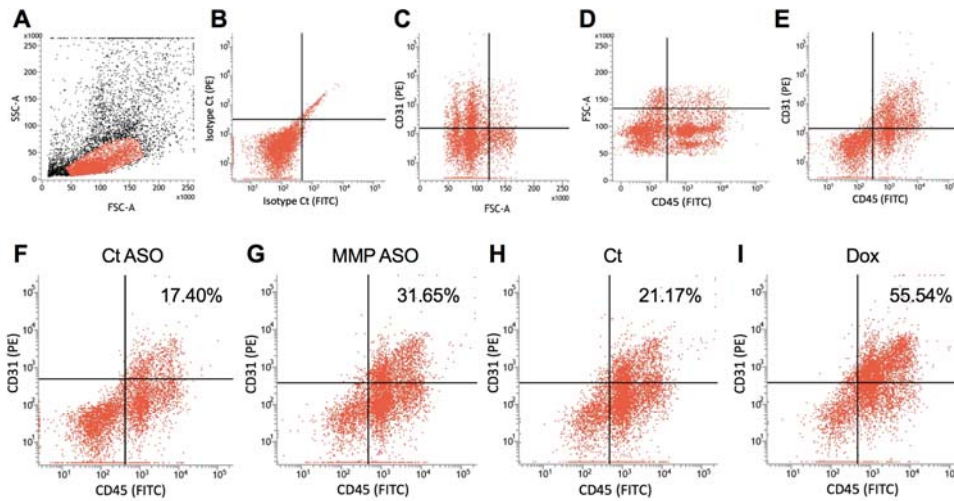
Supporting Figures S1-6

Supporting Tables S1-2

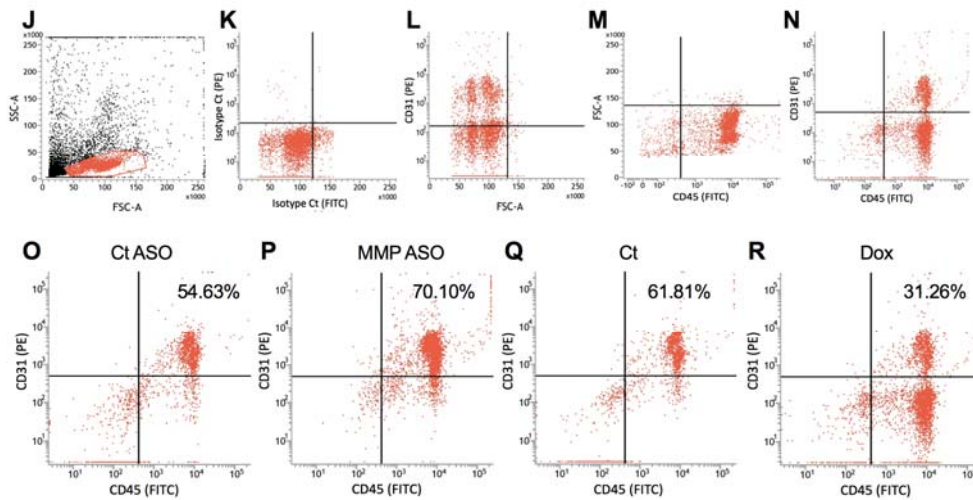
References

Supporting Figure S1

CD133+ Bone Marrow Cells



CD133+ Circulating Cells

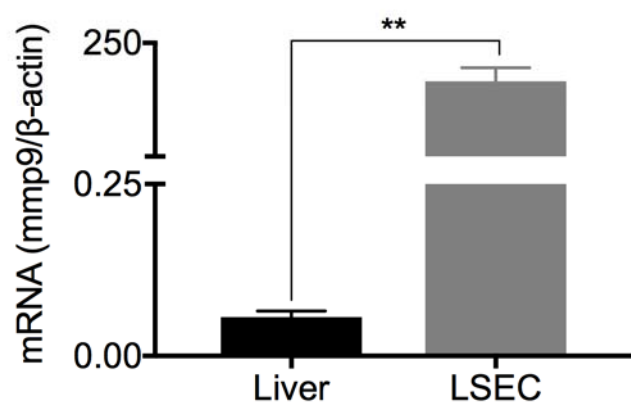


Supporting Figure S1: Representative images of Flow Cytometry assay of bone marrow and circulating sprocs. (A-I) Sorting of CD133+CD31+CD45+ bone marrow cells. **(J-R)** Sorting of CD133+CD31+CD45+ blood cells. Bone marrow or circulating mononuclear cells underwent positive selection with CD133 immunomagnetic beads using AutoMACS Pro, and then stained for CD31 (PE) and CD45 (FITC). Cell suspensions were sorted using the following gating strategy: **(A/J)** Target population was gated based on size x granularity and used for further analysis. **(B/K)** Quadrants were designed based on the isotype control staining (PE and FITC), which differentiated non-specific background signal from specific antibody signal. The presence of **(C/L)** CD31+ and **(D/M)** CD45+ populations was confirmed, and then the double positive cells were analyzed and quantified **(E/N)**.

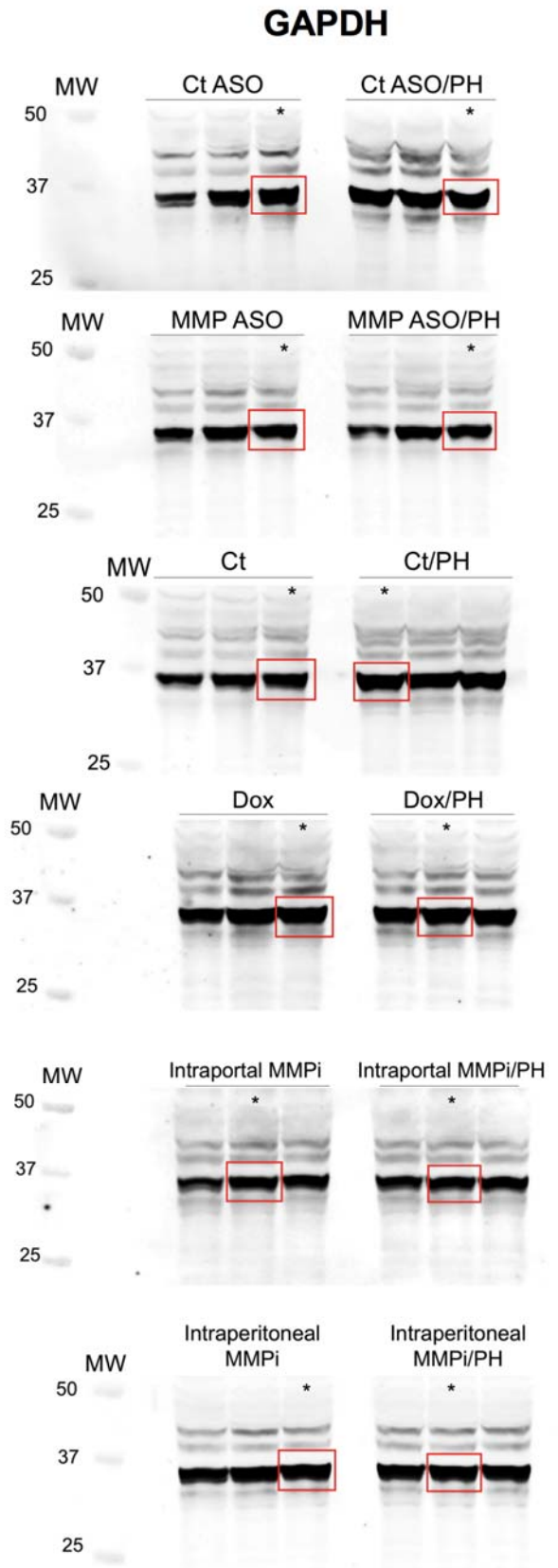
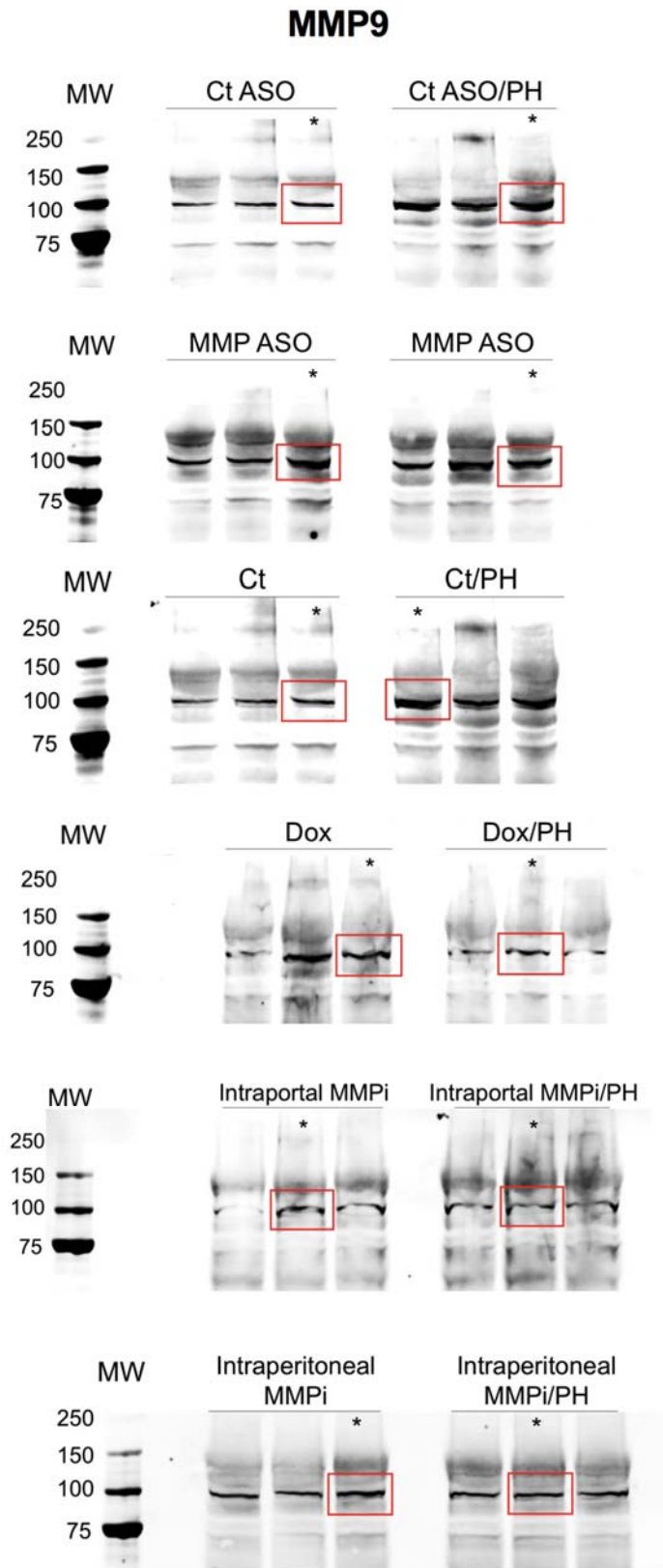
This analysis was performed in using animals treated with Ct ASO (**F/O**), MMP ASO (**G/P**), Ct (**H/Q**) and Doxycycline (**I/R**).

Supporting Figure S2A

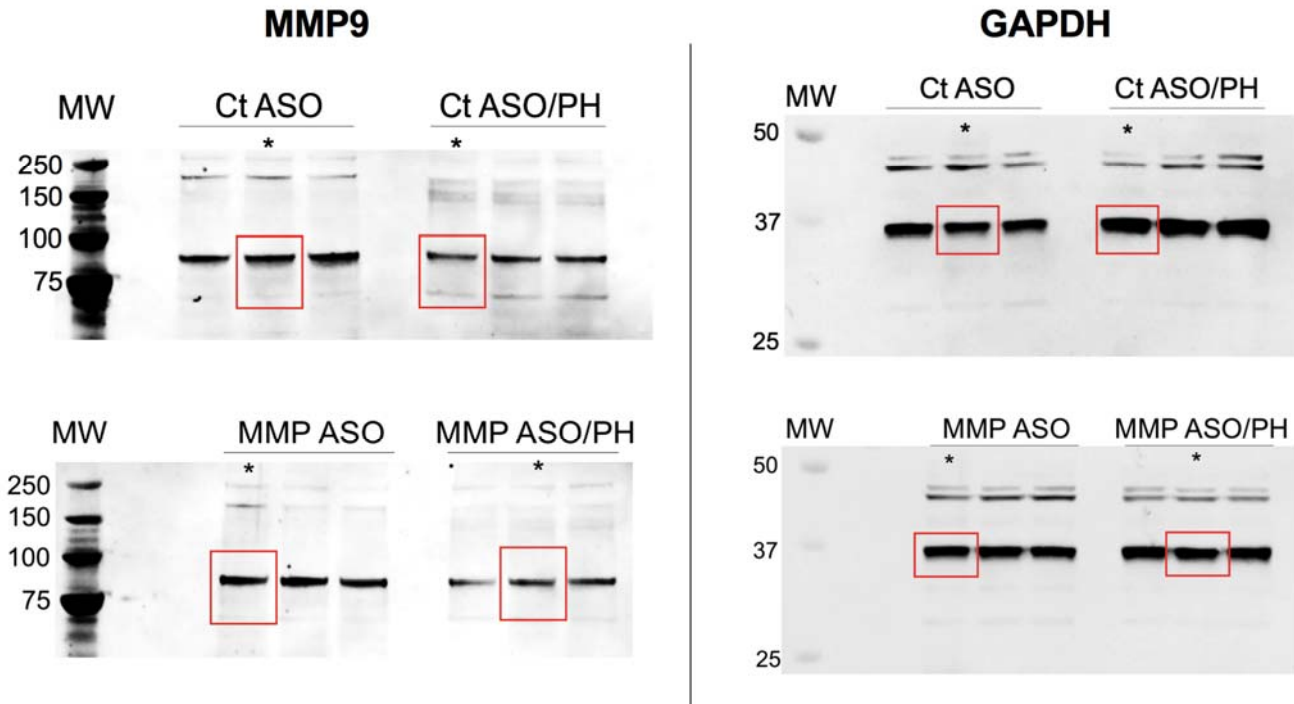
MMP-9 gene expression in
normal liver vs normal LSECs



Supporting Figure S2B



Supporting Figure S2C

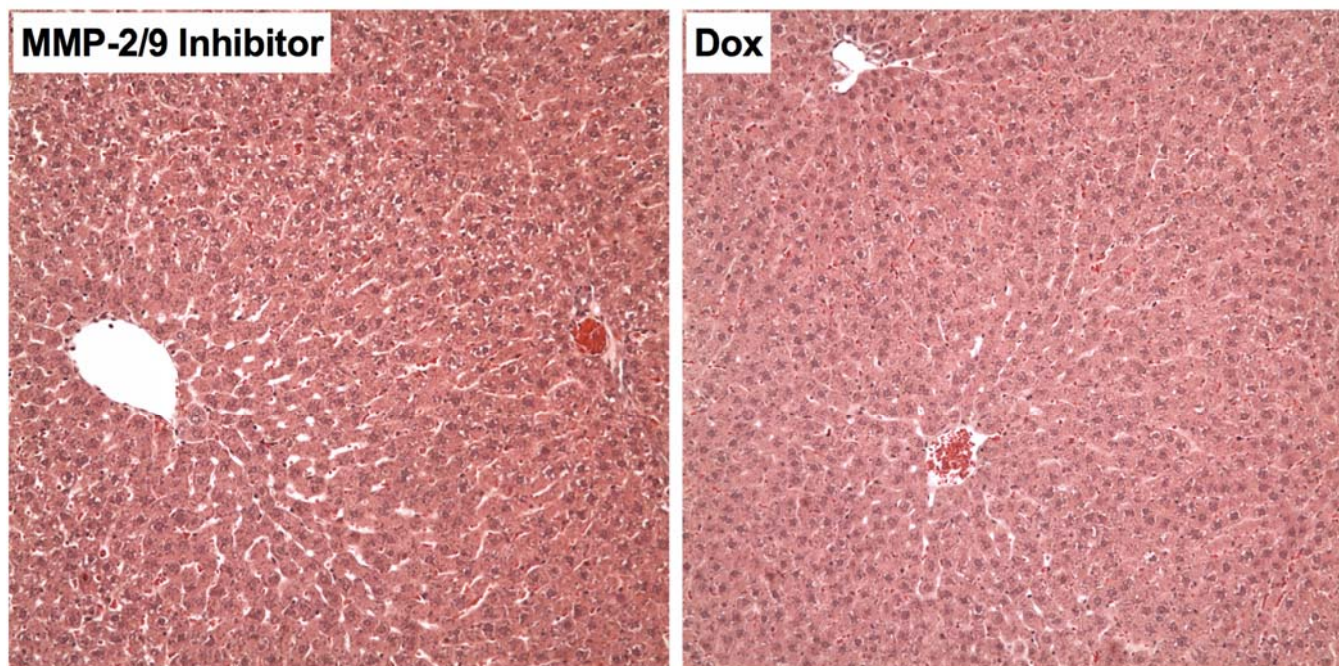


Supporting Figure S2A: LSEC is a major source of MMP-9 in the liver. MMP-9 gene expression was measured using RNA extracted from normal whole liver and from normal LSECs. LSECs express significantly higher levels of MMP-9 compared to whole liver, suggesting that LSECs are a major producer of MMP-9 in the liver. These results are consistent with our earlier findings, where we compared the gelatinolytic activity of LSECs, hepatocytes, Kupffer cells and HSCs in vitro, and showed that LSECs are the only significant source of MMP activity among these liver cells (1).

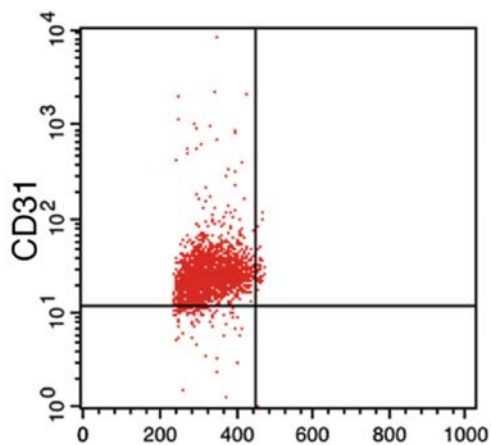
Supporting Figure S2B: Unprocessed original scans of Immunoblots related to Figure 1A. Uncropped images of all immunoblots. Red rectangles indicate portion of image used on indicated figure. Molecular size markers in kDa.

Supporting Figure S2C: Unprocessed original scans of Immunoblots related to Figure 1B. Uncropped images of all immunoblots. Red rectangles indicate portion of image used on indicated figure. Molecular size markers in kDa.

Supporting Figure S3A



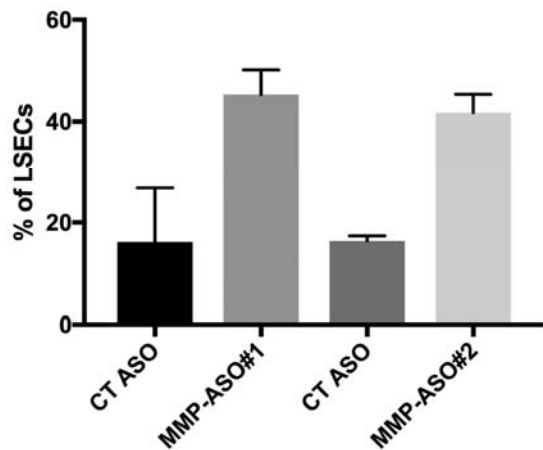
Supporting Figure S3B



Supporting Figure S3A: Cytotoxicity of MMP inhibitors. Histology showed no evidence of toxicity from the MMP-2/9 inhibitor or Doxycycline.

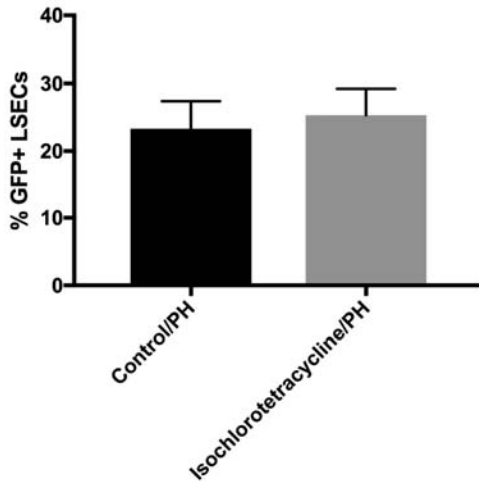
Supporting Figure S3B: CD31⁺ fraction of CD133⁺ liver cells. Whole liver was digested and CD133⁺ cells were isolated by immunomagnetic selection. Cells were stained for CD31. At least 94% of the CD133⁺ cells were CD31⁺.

Supporting Figure S4



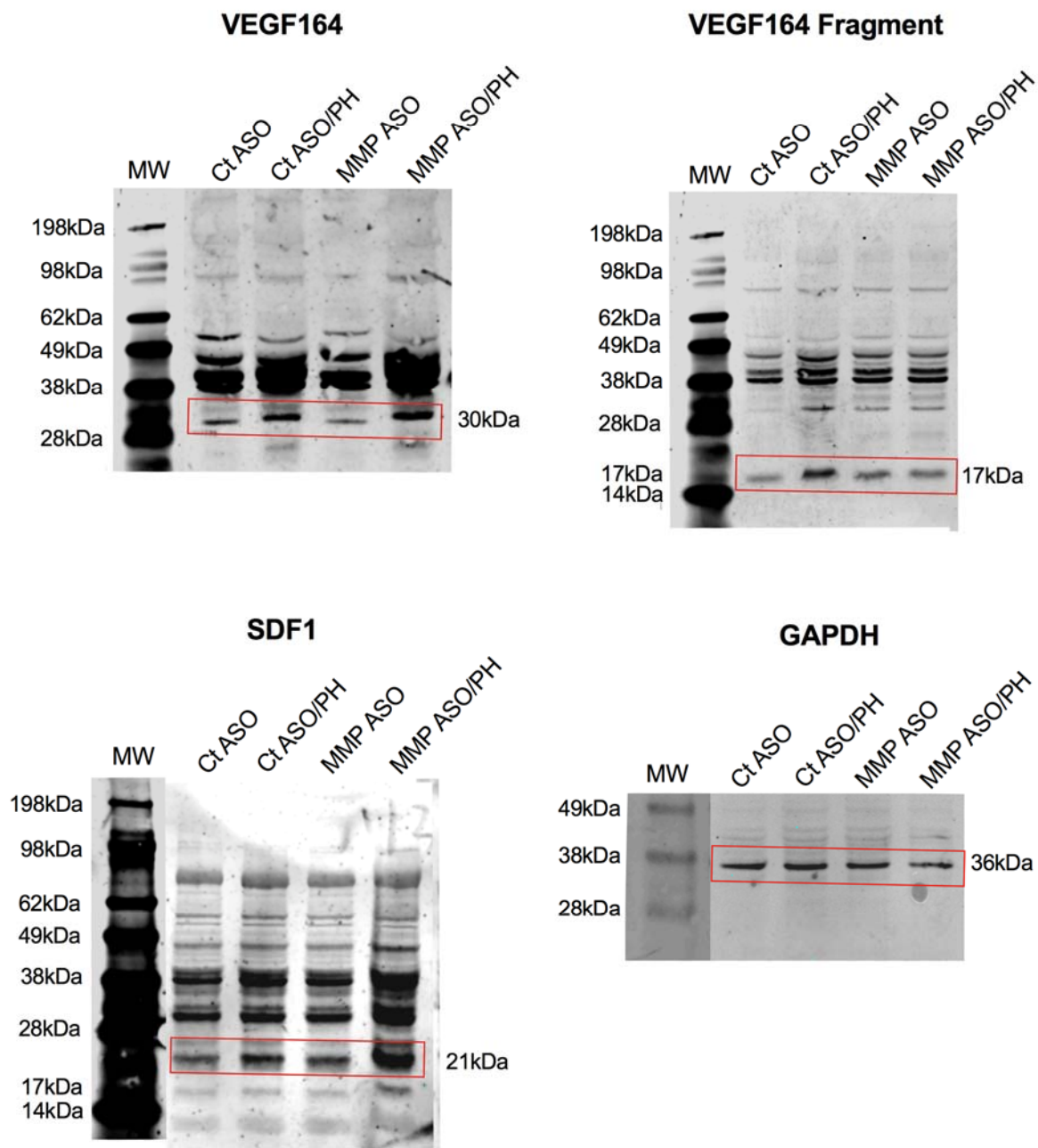
Supporting Figure S4: Confirmatory MMP-9 ASO. A second MMP-9 ASO was kindly provided by Ionis Pharmaceuticals to confirm that the effect of pretreatment with the MMP-9 ASO was through MMP-9 inhibition. There was no significant difference in engraftment of BM sprocs after PH between the effect of MMP-9 ASO #1 (also shown in Figure 4D) and a second MMP-9 ASO labeled MMP-9 ASO #2.

Supporting Figure S5



Supporting Figure S5: Effect of isochlorotetracycline pretreatment on BM sproc engraftment after partial hepatectomy. Isochlorotetracycline shares an antibiotic effect with doxycycline, but has only weak MMP inhibitory activity. Thus this is a control for the antibiotic effect of doxycycline on recruitment and engraftment.

Supporting Figure S6



Supporting Figure S6: Unprocessed original scans of Immunoblots related to Figure 5.

Uncropped images of all immunoblots. Red rectangles indicate portion of image used for figure 5. Molecular size markers in kDa.

Supporting Table S1. Antibodies used.

Antibody	Dilution	Vendor	Cat #
Fluorescein Iso-thiocyanate (FITC)-conjugated mouse anti-rat CD45	1:100	BD Biosciences	554877
Phycoerythrin (PE)-conjugated mouse anti-rat CD31	1:100	BD Biosciences	555027
Peridinin chlorophyll (PerCP)-conjugated mouse anti-proliferating cell nuclear antigen (PCNA)	1:100	Santa Cruz Biotechnology	SC-56PerCP
Mouse monoclonal anti-CD31	1:100	Santa Cruz Biotechnology	SC-376764
m-IgG κ BP-FITC anti-mouse IgG conjugate	1:500	Santa Cruz Biotechnology	SC-516140
Allophycocyanin (APC)- conjugated mouse anti-CXCR7/RDC1	1:100	R&D Systems	FAB8399A
Rabbit anti-Ki-67 antibody	1:50	Biocare Medical	CRM325A
MMP-9 antibody	1:500	Cell Signaling Technology	3852S
SDF1 antibody	1:250	Cell Signaling Technology	3740S
VEGF antibody	1:1000	Santa Cruz Biotechnology	SC-1836
GAPDH antibody	1:5000	Novus Biologicals	MB300-320
IRDye® 680LT Donkey anti-Rabbit IgG (H + L)	1:5000	Li-Cor Biosciences	925-68023
IRDye® 800CW Donkey anti-Goat IgG (H + L)	1:5000	Li-Cor Biosciences	925-32214

Supporting Table S2. Antisense oligonucleotide #1 Specificity

Oligo_ID	Oligo_Sequence	Database	Entrez Gene_ID	Gene Symbol	Accession	Position	Mismatch Count	Mismatch Annotation	Max Contig	Oligo Length	NCBI Sequence Viewer
Undefined	CCTCGTGGTAGTGATACATG	transcriptome_rat	81687	Mmp9	NC_005102.4_TRUNC_161413410_161421473	3112	0		20	20	View
Undefined	CCTCGTGGTAGTGATACATG	transcriptome_rat	304832	Cdc73	NC_005112.4_TRUNC_60403771_60496511_COMP	19734	2	3:C>G,9:C>T	10	20	View
Undefined	CCTCGTGGTAGTGATACATG	transcriptome_rat	309307	RGD1311595	NC_005100.4_TRUNC_247898572_247978661_COMP	17063	2	3:C>G,13:C>T	9	20	View
Undefined	CCTCGTGGTAGTGATACATG	refseq_rna_rat	81687	Mmp9	NM_031055.1	1266	0		20	20	View

The sequence of MMP-9 ASO#1 (ISIS-283953; 5'-CCTCGTGGTAGTGATACATG-3') was aligned against the rat transcriptome and mRNA reference sequences using the Bowtie Algorithm (2) for any sequences with 0 or one mismatch, or sequences with two mismatches and 18 consecutive matches. Previous experience has demonstrated that ASO are unlikely to have significant activity against transcripts with more than 2 mismatches (3-5). ASO#1 was the MMP ASO used throughout the study and no other gene fell into the category of a possible reduction.

Sequences of other antisense used for this study: MMP-9 ASO#2 (ISIS-283973; 5'-TGTCATGGCAGAAATAGGCC-3') and Scrambled control ASO (ISIS-141932; 5'-CCTTCCCTGAAGGTTCCCTCC-3').

NOTE: Both MMP-9 ASOs showed identical efficacy in promoting engraftment (supporting fig. S3), which is the result of the cumulative effects on bone marrow sproc proliferation, mobilization, and engraftment in the liver.

References:

1. DeLeve LD, Wang X, Tsai J, Kanel G, Strasberg S, Tokes ZA. Sinusoidal obstruction syndrome (veno-occlusive disease) in the rat is prevented by matrix metalloproteinase inhibition. *Gastroenterology* 2003;125:882-890.
2. Langmead B, Trapnell C, Pop M, Salzberg SL. Ultrafast and memory-efficient alignment of short DNA sequences to the human genome. *Genome Biol* 2009;10:R25.
3. Zhang H, Cook J, Nickel J, Yu R, Stecker K, Myers K, Dean NM. Reduction of liver Fas expression by an antisense oligonucleotide protects mice from fulminant hepatitis. *Nat Biotechnol* 2000;18:862-867.
4. Vickers TA, Koo S, Bennett CF, Crooke ST, Dean NM, Baker BF. Efficient reduction of target RNAs by small interfering RNA and RNase H-dependent antisense agents. A comparative analysis. *J Biol Chem* 2003;278:7108-7118.
5. Cioffi CL, Garay M, Johnston JF, McGraw K, Boggs RT, Hreniuk D, Monia BP. Selective inhibition of A-Raf and C-Raf mRNA expression by antisense oligodeoxynucleotides in rat vascular smooth muscle cells: role of A-Raf and C-Raf in serum-induced proliferation. *Mol Pharmacol* 1997;51:383-389.